*Particle Accelerators*
1975, Vol. 6, pp.175–182



# EXPERIMENTAL STUDY OF SPIRAL RESONATORS FOR ACCELERATION OF LOW VELOCITY IONS†

D. D. ARMSTRONG, P. J. BENDT, B. H. ERKKILA, J. S. LUNSFORD, J. P. SHIPLEY
R. H. STOKES, and J. SUTTON

*Los Alamos Scientific Laboratory, University of California, Los Alamos, New Mexico 87544, USA*

(*Received February 20, 1974; in final form November 22, 1974*)

The performance of copper spiral resonators operating at room temperature has been studied for possible applications in the acceleration of heavy ions. Many resonator models containing one, two, or three axially spaced spiral structures have been constructed and characterized at frequencies in the range 45–55, 80–84, and 99–106 MHz. Resonators with a variety of drift tube diameters have shunt impedance values in the range 30 to 74 megohms per meter. Six resonators have been tested at power levels of 10–20 kilowatts, and accelerating fields up to 2.6 megavolts per meter. The 100 MHz power source used in the experiments and the feedback control for amplitude, phase, and frequency are described. Natural alpha particles were accelerated with a three-spiral resonator and their energy gain was measured as a function of their detection time relative to the radiofrequency phase. The results of these tests show that spiral resonators have improved characteristics compared to short helix resonators of the same phase velocity.

## 1. INTRODUCTION

The recent increasing interest in heavy ion physics has emphasized the importance of constructing new heavy ion accelerators with improved characteristics. In the near future, beams of many heavy ion species having small energy spread, wide capability for energy variation, and other flexible beam properties will be required. An accelerator based on these objectives has been designed[1] and proposed for construction by the Los Alamos Scientific Laboratory. In this paper we report the development work performed on spiral resonator accelerating structures which are the basic element of the proposed facility. Spiral resonators, such as shown in Figure 1, were first described by Dick and Shepard,[2] who studied them in the superconducting form. Both the studies reported here and our proposed accelerator are based on the use of spiral resonators at room temperature. The proposed accelerator consists of an array of independently phased spiral resonators with the phase of each resonator adjusted to be optimum for the velocity of the ion to be accelerated. Magnetic quadrupole singlets placed between each resonator provide radial focusing.[3] The flexibility of such an arrangement is characteristically dependent upon the length of the individual resonators. To reduce the total number of independent resonators necessary to reach a specific final energy, it is desirable to use resonators with the greatest possible length consistent with the required flexibility. For this reason we have studied spiral structures which contain one, two, and three drift tubes with each tube supported on a separate spiral structure.

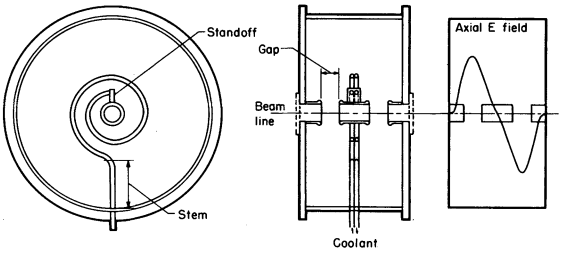


FIGURE 1 Schematic drawing of a 100 MHz λ/4 single spiral resonator. The axial accelerating E field extends into the drift tubes, and closely resembles a sine wave.

In this paper, we present the results of bead perturbation experiments on model resonators whose resonant frequencies ranged from 45 to 110 MHz. This is followed by a description of a 100 MHz power amplifier, and the feedback circuits used to follow the frequency shift and to

† Work performed under the auspices of the U.S. Atomic Energy Commission.

control mechanical instability during high power tests. The results of high power tests, and the acceleration of 5.48 MeV alpha particles from an Am-241 radioactive source are then described. In Section 6, we compare spiral resonators with helix resonators of $\lambda/2$ electrical length.[4]

## 2. LOW POWER MEASUREMENTS ON MODEL SPIRAL RESONATORS

A number of full scale copper model resonators have been assembled and tested at low rf power. The measurements consisted of finding the fundamental resonant frequency, measuring the $Q$, and measuring the shunt impedance by pulling a 3/16 in. diam sapphire bead along the cylindrical axis.[5] All the model resonators were built with active drift tubes mounted on the spirals, and most of the resonators had electrically grounded drift tubes of the same diameter mounted on the end plates. The resonant frequencies changed with every modification in geometry, but were primarily determined by the lengths of the spirals. Thus, the 145 cm-long quarter wavelength ($\lambda/4$) spirals resonated near 50 MHz; the 110 cm-long spirals near 70 MHz; the 95 cm-long spirals at about 83 MHz; and 75 cm-long spirals at about 100 MHz. When two and three spirals were mounted on the same cylindrical shell, the resonant frequency was lower due to mutual inductive and capacitive coupling.

The performance and dimensions of 22 resonators are listed in Table I and will be discussed by groups. Groups 1, 2, and 3 give the performance of single $\lambda/4$ spiral resonators, whose resonant frequencies fall in three ranges, and group 4 describes two resonators with very small drift tubes. These latter resonators have unusually high shunt impedances, 64 and 75 MΩ/m, but the drift tubes have apertures which may be too small for use in some types of accelerators. Group 5

TABLE I

Performance and dimensions of copper spiral resonators

| Group | No. of Spirals | Phase Velocity (v/c) | Resonant Frequency (MHz) | Shunt Impedance MΩ/m | $Q$ | Spiral Tubing Diam. (cm) | Drift Tube Rad. (cm) | Drift Tube Length (cm) | Outside Shell Rad. (cm) | Outside Shell Length (cm) |
|---|---|---|---|---|---|---|---|---|---|---|
| 1 | 1 | 0.016 | 51.1 | 43 | 2300 | 0.95 | 1.9 | 2.5 | 16.2 | 12.7 |
| | 1 | 0.027 | 54.9 | 44 | 2520 | 0.79 | 1.9 | 6.4 | 16.2 | 12.7 |
| | 1 | 0.040 | 48.9 | 39 | 2850 | 0.79 | 1.9 | 10.2 | 16.2 | 22.9 |
| | 1 | 0.066 | 45.0 | 17 | 2210 | 0.79 | 1.9 | 20.3 | 16.2 | 38.1 |
| 2 | 1 | 0.021 | 80.5 | 32 | 2200 | 0.95 | 1.9 | 3.0 | 12.6 | 10.2 |
| | 1 | 0.033 | 83.2 | 39 | 2380 | 0.95 | 1.9 | 4.6 | 12.6 | 12.7 |
| | 1 | 0.044 | 84.3 | 36 | 2390 | 0.95 | 1.9 | 6.2 | 12.6 | 15.2 |
| | 1 | 0.067 | 84.4 | 25 | 2430 | 0.95 | 1.9 | 10.0 | 12.6 | 22.9 |
| 3 | 1 | 0.035 | 106.2 | 41 | 2120 | 0.79 | 1.9 | 2.9 | 16.2 | 11.2 |
| | 1 | 0.045 | 99.2 | 37 | 2670 | 0.95 | 1.9 | 5.1 | 16.2 | 12.7 |
| | 1 | 0.062 | 104.9 | 32 | 2570 | 0.95 | 1.9 | 6.8 | 12.6 | 15.2 |
| | 1 | 0.083 | 101.3 | 28 | 2430 | 0.79 | 1.9 | 10.2 | 12.6 | 17.8 |
| 4 | 1 | 0.016 | 99.5 | 75 | 2460 | 0.48 | 0.54 | 1.5 | 7.5 | 6.4 |
| | 1 | 0.027 | 99.7 | 64 | 2250 | 0.64 | 0.75 | 0.95 | 16.2 | 11.2 |
| 5 | 1 ($\lambda/2$) | 0.025 | 49.5 | 44 | 2300 | 0.79 | 1.9 | 6.4 | 16.2 | 12.7 |
| | 1 ($\lambda/2$) | 0.055 | 50.4 | 30 | 2940 | 0.79 | 1.9 | 15.2 | 16.2 | 22.9 |
| 6 | 2 opposed | 0.023 | 49.5 | 51 | 2080 | 0.79 | 1.9 | 5.1 | 16.2 | 20.3 |
| | 2 same | 0.026 | 55.4 | 45 | 2030 | 0.79 | 1.9 | 5.1 | 16.2 | 20.3 |
| 7 | 3 opposed | 0.026 | 97.0 | 40 | 2070 | 0.79 | 1.9 | 2.3 | 16.2 | 17.8 |
| | 3 opposed | 0.037 | 70.2 | 48 | 2550 | 0.95 | 1.9 | 6.0 | 16.2 | 30.1 |
| | 3 opposed | 0.052 | 110.6 | 42 | 2580 | 0.95 | 1.9 | 4.0 | 16.2 | 30.1 |
| | 3 opposed | 0.084 | 97.5 | 28 | 2280 | 0.79 | 1.9 | 8.5 | 16.2 | 53.3 |

describes two resonators containing half wavelength ($\lambda/2$) spirals which are grounded at both ends and support the active drift tube at the electrical midpoint. This design has the advantage of supporting the drift tube symmetrically.

Group 6 consists of resonator geometries containing two axially spaced $\lambda/4$ spirals in one shell. The spirals were the same in both resonators, the only difference being that the spirals were first installed with the windings opposed (left-handed and right-handed), and the second time with the windings in the same direction. With the windings opposed, the frequency was lower and the shunt impedance was higher, because of the increased mutual inductance. Group 7 consists of resonators containing three axially spaced $\lambda/4$ spirals. The spirals were mounted with the center spiral opposed to the two end spirals as shown in Figure 2.

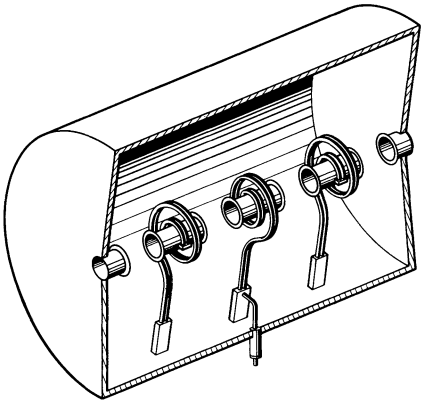

FIGURE 2 Schematic drawing of resonator E, containing three axially spaced coupled spirals. The center spiral is opposed to the end spirals in order to increase the mutual inductive coupling.

The shunt impedances of the resonators contained in groups 1, 2, 3 and 7 have been plotted as a function of phase velocity in Figure 3, along with a few additional resonators in the same frequency ranges. The single-spiral curves in Figure 3 show that the 45–55 MHz resonators have higher shunt impedance at phase velocities less than 0.026, while the 99–106 MHz resonators are superior for phase velocities greater than 0.05. The curves also show that resonators with three coupled spirals have substantially higher shunt impedance than single-spiral resonators of the same frequency in the phase velocity range between 0.026 and 0.052.

We have empirically determined that the best

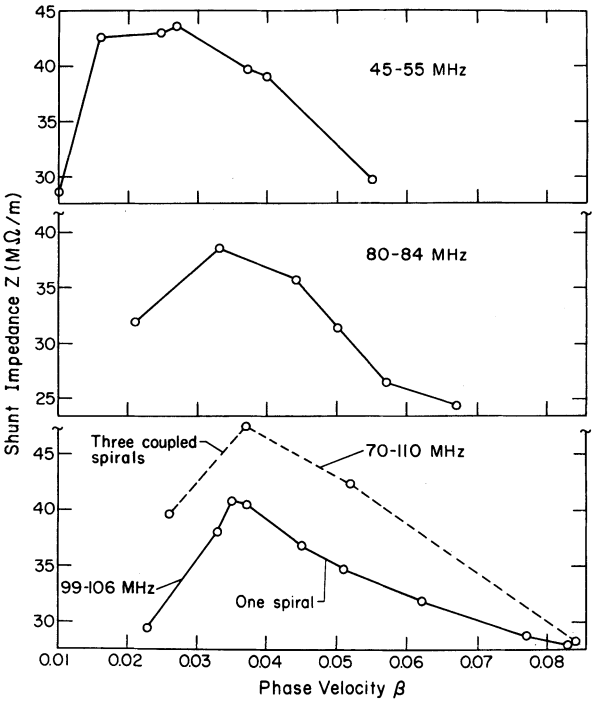


FIGURE 3 The shunt impedance of single spiral resonators in three frequency ranges, and of three-spiral resonators operating in the 70–110 MHz range.

shunt impedance is obtained with 100 MHz $\lambda/4$ spirals if the tubing extends radially inward for about 8 cm (one-half the shell radius) before the spiral is wound (Figure 1). The tubing is then wound in a comparatively tight spiral of $1\frac{1}{4}$ to $1\frac{3}{4}$ turns, until the inner radius is about twice the drift tube radius. The spirals were wound with a uniform center to center spacing between turns, which was typically 2.8 times the tubing diameter. A standoff is attached to the inner end of the spiral to support the drift tube, which is coaxial with the outer cylindrical shell. The 50 MHz resonators were constructed with the same size outer cylinders, but with shorter radial stems (4 cm), and the conductor was wound into a $2\frac{1}{2}$ to 3 turn spiral.

A measurement was made of the relative rf current along a 70 MHz $\lambda/4$ spiral, and the results are shown in Figure 4. The measurement was made by sliding a ferrite toroid along the spiral and measuring the $Q$ and resonant frequency for successive positions of the toroid. The $Q$ is reduced by the energy dissipated in the ferrite, which is proportional to the square of the rf current passing through the toroid. The following equation was used to calculate the relative current $I(x)$ at

position $x$ along the spiral:

$$I(x) = A\left[\frac{1}{Q(x)} - \frac{1}{Q_0}\cdot\frac{f_0}{f(x)}\right]^{1/2}, \qquad (1)$$

where $A$ is a constant, $f$ is the resonant frequency, and $Q_0$ and $f_0$ refer to values with the toroid removed. The current distribution approximates a cosine function between 0 and $\pi/2$. The dip at the left end of the "cosine" distribution is associated with the radial stem which supports the spiral turns, and the bulge at the right end disappears if the drift tube is replaced by a thin ring of the same diameter.

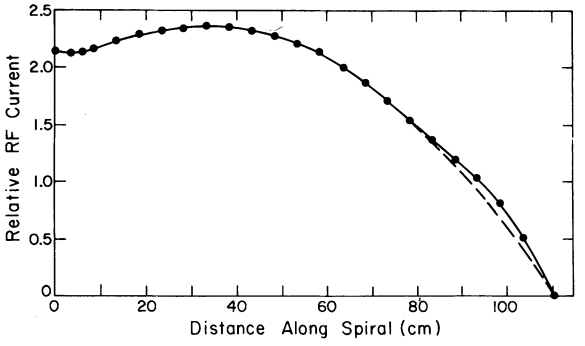


FIGURE 4 The rf current distribution along a 110 cm long spiral in a 70 MHz resonator. The spiral was attached to the outer cylinder at zero on the horizontal scale, and the drift tube was attached at 110 cm.

## 3. POWER AMPLIFIER AND FEEDBACK CONTROLS

An amplifier was constructed to permit the testing of spiral resonators at power levels up to 25 kW.[6] The final stage operated in the Class A mode and was tunable from 94 to 106 MHz. A 50-Ω coaxial line, appropriately matched to the amplifier plate circuit, delivered rf power to a spiral resonator. During operation, the amplitude of the resonator electric field, the rf phase of the resonator, and the operating frequency were controlled by electronic feedback circuits.

A block diagram of the complete amplifier and control system is shown in Figure 5. The amplitude control was capable of damping mechanical vibrations in the range 100 to 400 Hz, which tend to occur at high power levels. This was accomplished by a feedback signal to the screen supply of the final-stage tetrode. The amplitude control had a band width of about 1 kHz and a stability better than one per cent.

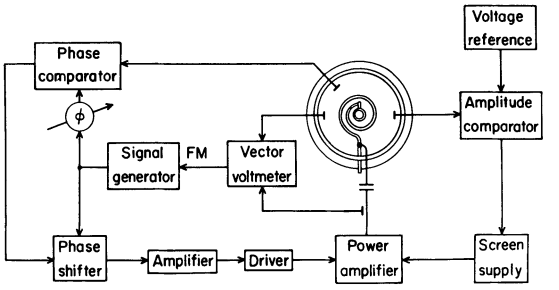


FIGURE 5 Block diagram of the power amplifier, spiral resonators, and control systems.

To determine if the phase control requirements could be met for an array of independently phased resonators, a phase control loop was constructed. The signal generator and resonator phase were compared in a balanced mixer, and the resulting error was applied to a 360 degree electronically controlled phase shifter placed between the signal generator and the power amplifier. The band width of the system was about 12 kHz, and the control accuracy was about 0.1 degree.

For testing single resonators, it was sufficient to provide a control which maintained the signal generator at the fundamental resonant frequency of the resonator. This was done by using a vector voltmeter to measure the phase difference between the rf power applied to the resonator and a signal derived from a probe inside the resonator. This error signal was connected to the frequency modulation input of the Hewlett-Packard 608F signal generator. The frequency control loop had a small bandwidth (10 Hz) which was characteristic of the vector voltmeter, but this was sufficient to maintain resonance conditions in the presence of varying power levels and other perturbing factors.

## 4. HIGH POWER TESTS ON SPIRAL RESONATORS

Six spiral resonators were tested at rf power levels of 10 kW or more, and the results of the tests are summarized in Table II. Power was delivered to the resonators by a $1\frac{5}{8}$ in. diam 50-Ω coaxial cable. The center conductor delivered rf power to a series capacitor, which was connected through a ceramic feedthrough to a magnetic coupling loop inside the resonator. The capacitor and loop were adjusted so that the resonator had a 50-Ω resistive input impedance at the resonant frequency. The resonators were water cooled and evacuated to $10^{-6}$ Torr with a turbomolecular pump.

TABLE II

Results of high power tests on spiral resonators. The shunt impedances are those obtained from bead perturbation measurements

| Designation | Spirals | Design | Resonant Frequency (MHz) | Phase Velocity (v/c) | Impedance (MΩ/m) | Frequency Shift (kHz/kW) | Maximum rf Power (kW) | Maximum Accel. Field (MV/m) |
|---|---|---|---|---|---|---|---|---|
| A | 1 | Figure 1 | 54.9 | 0.027 | 43.5 | −5.2 | 10 | 1.8 |
| B | 1 | Figure 6 | 50.2 | 0.025 | 42.9 | −6.1 | 20 | 2.6 |
| D | 1 | λ/2 spiral | 50.4 | 0.055 | 29.7 | −51 | 10 | 1.1 |
| E | 3 | Figure 2 | 98.4 | 0.052 | 39.2 | −32 | 12 | 1.2 |
| F | 3 | Figures 2, 7 | 94.9 | 0.049 | 38.3 | −16 | 20 | 1.5 |
| G | 1 | Figure 1 | 102.4 | 0.050 | 26.5 | −17 | 10 | 1.3 |

The first two power resonators (A and B) were tested before the amplitude control circuit mentioned in Section 3 was built, so the maximum power was limited by the onset of mechanical oscillations of the spiral. The difference between these two resonators was in the arrangement of the two pieces of 5/16 in. copper tubing which formed the spiral and provided water cooling for the drift tube. These were brazed side by side axially in resonator A (Figure 1), while they were positioned in the radial plane in resonator B (Figure 6). An average axial field of 2.6 MV/m was reached while testing resonator B without the use of feedback control circuits. No attempt was made to determine the maximum axial field at which the resonators would operate. However, at the power levels used, no breakdown or multipactoring phenomena were observed.

The half-wavelength spiral in resonator D was wound of copper-plated 5/16 in. type 304 stainless steel tubing. Since λ/2 spirals are grounded at both ends, the spiral was formed of single rather than double tubing and was less rigid than the λ/4 spirals. Without an amplitude control circuit, the resonator would not absorb power due to mechanical oscillations of the spiral. With the control circuit in operation, the spiral was stabilized, and the resonator was tested up to 10 kW. The large negative frequency shift with increasing rf power is attributed to the flexibility of this particular spiral design.

Resonator E contained three axially spaced spirals in the geometry shown in Figure 2. The active drift tubes and the gaps were each 4 cm long, and the amplitude of the accelerating fields in the gaps had relative values 1, −2, 2, −1. This resonator also had a large frequency shift with increasing rf power, which is attributed to unbalanced axial forces on the end spirals. Resonator F contained the same spirals, but the outer drift tubes were lengthened so that the two outside gaps were 2 cm, while the center gaps were 4 cm. The location of the midplanes of all four gaps was not changed, but the increased capacitive coupling to ground lowered the resonant frequency, and thus reduced the phase velocity. In resonator F, the maximum accelerating fields in the gaps had relative values 1, $-\sqrt{2}$, $\sqrt{2}$, 1. The forces on the end spirals

FIGURE 6 Photograph of resonator B with the end plates removed. A 120 pF vacuum coupling capacitor is shown at the top of the figure. This resonator was operated at 2.6 MV/m without the use of feedback control circuits.

were more nearly balanced, and the frequency shift with increasing rf power was reduced to one-half of that in resonator E. The relative gap dimensions and the measured axial electric field are shown in Figure 7.

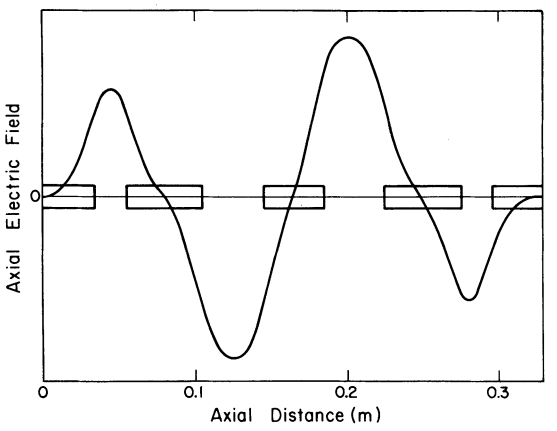


FIGURE 7 The measured axial electric field in resonator F, with gaps between drift tubes of 2, 4, 4, and 2 cm. The amplitudes of the fields in the gaps had relative values 1, $-\sqrt{2}$, $\sqrt{2}$, $-1$.

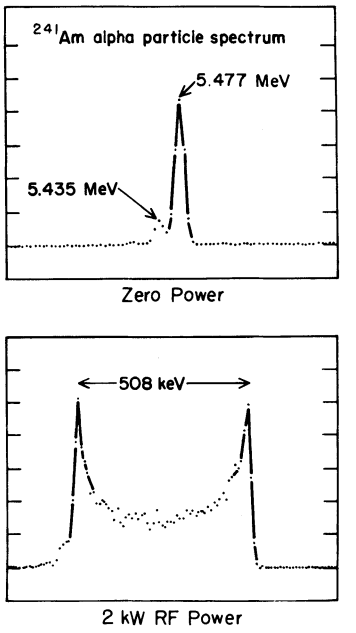


FIGURE 8 Energy spectra of $^{241}$Am alpha particles which have traveled through resonator E.

## 5. ACCELERATION OF ALPHA PARTICLES

The principal alpha particle peak (Figure 8) from an $^{241}$Am radioactive source has an energy of 5.477 MeV, corresponding to a velocity of 0.054 c. Since this velocity falls near the center of the range of heavy ion velocities for which the proposed accelerator was designed, the acceleration of $^{241}$Am alpha particles was a useful test of the performance of spiral resonators. Three kinds of information were provided by the measurements. First, the energy gain of the alpha particles when used with a computed transit time factor gave an independent measurement of the resonator shunt impedance. Second, the time-resolved, phase-related energy gain and loss of the alpha particles gave a detailed look at the acceleration mechanism of a beam traversing the resonator. Third, we observed particle bunching effects consistent with predictions.

Resonators E and F (Table II) were used to accelerate alpha particles, and resonator G was used in a bunching experiment. Two radioactive sources were purchased from Amersham/Searle.[7] The 13 μCi source had a FWHM energy spread of 15 keV, and the 100 μCi source had an energy spread of 30 keV. The energy of alpha particles was measured with Ortec[8] silicon surface barrier detectors. In order to make acceleration measurements, a source was mounted on one end-plate of a three-spiral resonator, and the detector was mounted at the end of a beam tube, 13 cm beyond the other end-plate. A 3 kG permanent magnet was mounted between the resonator and detector and served as an electron trap. In Figure 8, we show the alpha energy spectrum obtained with resonator E as displayed on the pulse height analyzer with the rf power turned off, and with the resonator excited with 2 kW of power. Due to the random phase with which alpha particles entered the resonator, a symmetric energy gain and energy loss spectrum is obtained. The linearity of the energy gain squared with rf power is shown for resonator F in Figure 9. The slope of the straight line is proportional to $ZT^2$, where $Z$ is the bare shunt impedance of the resonator, and $T$ is the transit time factor. The transit time factor was calculated by a computer code which used the measured field distribution shown in Figure 7. From alpha particle energy gain measurements (Figure 9) and calculated transit time factors, values of $Z$ were obtained and they are listed in Table III, along with the corresponding bead perturbation measurements. We have corrected the alpha energy gain for resolution effects arising from the 15 keV energy spread of the alpha particle source.

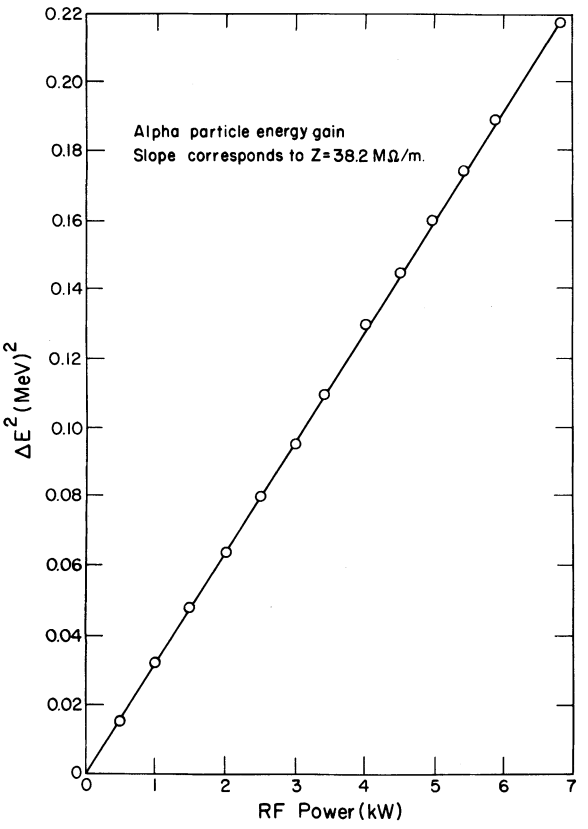


FIGURE 9 The square of the alpha particle energy gain, plotted against rf power, for resonator F. Each point is obtained from a time-integrated energy spectrum similar to that shown in Figure 8.

The good agreement between the two methods demonstrates the reliability of the many shunt impedance values which we determined by the bead perturbation method.

For resonator F, we recorded time-resolved measurements of the alpha particle energy gain and loss at 2 kW, which are shown in Figure 10. One period was 10.5 ns long, and the counting gates were ~0.8 ns wide. Due to the 30 cm drift distance between the midpoint of the resonator and the detector, the computer-calculated curve in Figure 10 is not quite a sine wave. Since accelerated alpha particles arrive early, and decelerated particles arrive late, the slopes of the linear portions of the curve are different, in agreement with the measured points.

TABLE III

Comparison of shunt impedance based on alpha particle energy gain, with those obtained from bead perturbation measurements, for three resonators listed in Table II. $T$ is the transit time factor.

| Resonator | E | F | G |
|---|---|---|---|
| Computed $T^2$ | 0.659 | 0.661 | 0.575 |
| $ZT^2$ from alpha energy gain, MΩ/m | 25.7 | 25.2 | 14.3 |
| Alpha energy gain $Z$, MΩ/m | 39.1 | 38.2 | 24.9 |
| Bead Perturbation $Z$, MΩ/m | 39.2 | 38.3 | 26.5 |

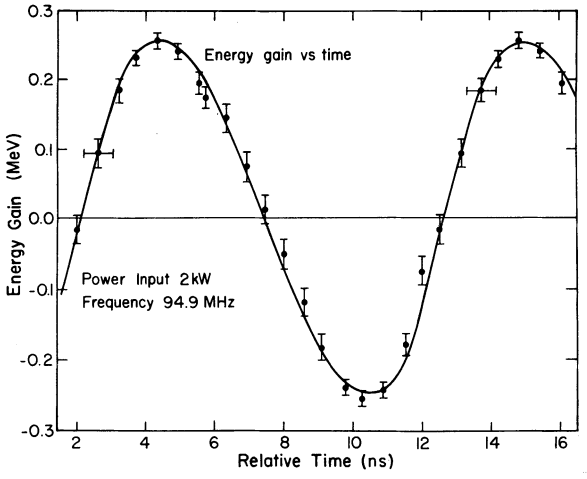


FIGURE 10 The time-resolved, phase-related alpha particle energy distribution from resonator F excited with 2 kW rf power. The energy baseline corresponds to the incident alpha energy of 5.477 MeV. One period is 10.5 ms, and time along the abscissa is measured from a trigger pulse derived from the rf field in the resonator.

An extension of the above experiment was performed to test the bunching capability of a single drift tube resonator. A drift space of 1.3 m was used and the alpha particles were focused on the detector with a quadrupole triplet magnetic lens. Within the timing capability of the detection system (1.5 ns), the observed bunching agreed with the beam dynamics calculations, which indicated that about 30 per cent of the dc beam could be concentrated within a 0.5 ns interval.

## 6. COMPARISON WITH HELIX RESONATORS

Previous to this investigation we had carried out a program of design and improvement of helix resonators with $\lambda/2$ electrical length.[4] With only intuitive guidance we constructed a first spiral resonator, and with no adjustment its shunt impedance was higher than any of the helix resonators. This higher efficiency continues to be a

characteristic of spiral resonators and at the same time they have other properties which are improvements on the $\lambda/2$ helix. One of these is the independent control of the axial field distribution through design of the drift tube arrangement. In this way one can optimize accelerating fields in a manner substantially independent of the spiral structure, which predominantly controls the electrical characteristics and the rigidity. The mechanical rigidity is superior because the space available for the spiral permits use of a larger diameter conductor. In our present work we have not always optimized the rigidity, and further improvement should be possible. This increased rigidity minimizes the requirements of the feedback control systems used to prevent mechanical oscillations, and may be particularly important in superconducting applications. Also, in contrast to the helix, the larger conductor permits the use of normal pressure to provide coolant water flow. Finally, the spiral resonator as well as the helix has small transverse dimensions which makes it particularly adaptable for use in modular assemblies of independently phased resonators.

## 7. ACKNOWLEDGEMENTS

We gratefully acknowledge many helpful discussions with Professor T. Tombrello, Dr. A. Sierk, Dr. J. Dick, and Dr. K. Shepard, all at the California Institute of Technology. We also acknowledge the assistance of Mr. J. Doherty, a consultant to the Los Alamos Scientific Laboratory, who participated in the design and construction of the rf power amplifier.

## REFERENCES

1. R. H. Stokes and D. D. Armstrong, Design Studies of heavy ion linear accelerators constructed of independently phased spiral resonators, (LASL report, in preparation)
2. G. J. Dick and K. W. Shepard, *Appl. Physics Lett.* **24**, 40 (1974).
3. D. D. Armstrong and W. S. Hall, Computer programs for the analysis of heavy-ion linear accelerator beam dynamics, (LASL report, in preparation).
4. P. J. Bendt, B. H. Erkkila, and R. H. Stokes, *Nucl. Inst. and Methods* **116**, 555 (1974).
5. P. J. Bendt, A. J. Sierk, and T. A. Tombrello, Field distributions in a spiral resonator, *Nucl. Inst. and Methods* (to be published); E. L. Ginzton, *Microwave Measurements* (McGraw-Hill Book Co., Inc. New York, 1957) Chapter 10.
6. J. S. Lunsford, P. J. Shipley, and J. Sutton, 100 MHz power amplifier design and control for a heavy ion accelerator (LASL report, in preparation).
7. Amersham/Searle Corp., Arlington Heights, Illinois 60005.
8. Ortec, Inc. (E. G. & G), Oak Ridge, Tenn. 37830.